

# Fourier family match on an elastic rectangle under its own weight

M. Bednárík, I. Kohút

Geophysical Institute of the Slovak Academy of Sciences<sup>1</sup>

**Abstract:** Surfaces of many structures in the scope of earth sciences contain sharp edges and corners where mechanical stress concentrates, and where not only the real material but also the mathematical methods of displacement or stress field investigation are most likely to fail, or, as for the latter, to have at least some difficulties. How do the methods of the Fourier family perform in such situations? We gathered some of them for a friendly match in solving the 2D biharmonic problem in a linearly elastic rectangle under its own weight. The prize is quite strange – the winner shall become a referee for future (mis)matches with other methods like finite element method.

**Key words:** plane strain, biharmonic equation, method of homogeneous solutions, method of superposition

## 1. Introduction

In our studies of the cavity effect and deformation of speleothems, we were often looking at the results of plane strain finite element method (FEM) computations with quite a big deal of mistrust. Is that islet of unexpected values a real thing or just an artifact? There are various methods to estimate the error in discrete methods, but, as we think, the most persuasive means is the direct comparison with the analytical reference solution. Of course, for complicated geometries, it is too hard to find. So, we have to find a domain easy to describe, nevertheless interesting enough, for which we can find the analytical solution(s) of our problem, make comparisons with FEM, and take lessons before going to more realistic geometries. The rectangle is an ideal playground, for a long time and often visited, yet still interesting (*Meleshko, 1995*).

In many civil engineering textbooks on linear elasticity, too many times some magic sentences like “according to the Saint-Venant principle” or

---

<sup>1</sup> Dúbravská cesta 9, 845 28 Bratislava, Slovak Republic  
e-mail: geofmabe@savba.sk; geofkohi@savba.sk

“let us neglect the own weight of the beam” appear in solved examples. (Un)fortunately, in geoscientific linear elasticity problems, the neglect of gravity is rarely possible. Own weight is, however, really not a thing to be afraid of. In fact, the own weight problems are, as we will show, a nice example of those where polynomials can be very helpful.

## 2. A fair match

Before introducing in detail the analytical methods of the Fourier family used here, we have to say, that they are approximate and discrete in some sense as well. From the point of view of signal processing theory, they are based on sampling (and then reconstructing) of the continuous functions (from samples taken) at fixed points in the frequency domain.

Whichever Fourier method we use, it will necessarily lead to solving a finite system of linear algebraic equations, as it is in ‘purely’ discrete methods.

Not the number of unknowns but the *number of rows* of the system – the same as number of samples – is the most important criterion of the fairness of the contest between different methods. Indeed, of the information available, Fourier methods first process as big a part as possible analytically. The remainder of the information has to be sampled and the amount of this discrete information – the number of samples – has to be kept constant in all the methods.

After the back-substitution of the Fourier series coefficients found by the solution of the linear system, we obtain an analytical approximation to the solution of the problem. It differs from the ideal solution due to the combined (acting against each other) effects of the omission of the terms *out* of the frequency range of our interest, and a partial compensation of their input to the solution by slightly wrong (with respect to the ideal solution) values of coefficients with the terms *within* our frequency range.

## 3. The statement of the problem

Let us have an isotropic linearly elastic body, characterized by density  $\rho$ , Young modulus  $E$ , and Poisson number  $\nu$ , in the form of rectangular par-

allelepip of infinite length and of rectangular perpendicular cross-section with dimensions  $2a \times 2b$ . Let us have gravity  $\vec{g} = \{g_x, g_y, g_z\}$  perpendicular to two of its faces with the width  $2a$  (Fig. 1). Into the center of a cross-section, we introduce a cartesian coordinate system with  $z$ -axis parallel to the length of parallelepiped and  $y$ -axis parallel to  $\vec{g}$ . With this setting, of  $g_x, g_y, g_z$  only  $g_y \neq 0$  and we will denote it  $g$ . Satisfying the (to be given later) boundary condition, we shall find displacements in  $x$  and  $y$  directions  $u_x, u_y$  and stresses  $\tau_{xx}, \tau_{yy}, \tau_{xy}$  in the rectangular cross-section perpendicular to  $z$ .

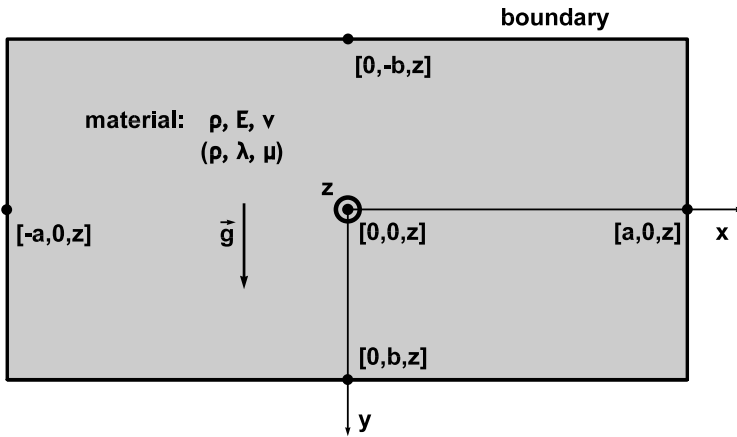


Fig. 1. The rectangular cross-section and the coordinate system setting.

This is the *plane strain problem*, for which

$$\varepsilon_{xz} = 0, \quad \varepsilon_{yz} = 0, \quad \varepsilon_{zz} = 0, \quad \tau_{xz} = 0, \quad \tau_{yz} = 0, \quad \tau_{zz} = \nu(\tau_{xx} + \tau_{yy}) \neq 0$$

where  $\varepsilon_{ij}$  and  $\tau_{ij}$  are components of the strain and stress tensors, respectively.

The remaining stresses have to satisfy the equations of equilibrium in  $x$  and  $y$  direction, respectively:

$$\frac{\partial \tau_{xx}}{\partial x} + \frac{\partial \tau_{xy}}{\partial y} = 0, \quad \frac{\partial \tau_{xy}}{\partial x} + \frac{\partial \tau_{yy}}{\partial y} + \rho g = 0, \tag{1}$$

As

$$\varepsilon_{xx} = \frac{\partial u_x}{\partial x}, \quad \varepsilon_{yy} = \frac{\partial u_y}{\partial y}, \quad \varepsilon_{xy} = \frac{1}{2} \left( \frac{\partial u_x}{\partial y} + \frac{\partial u_y}{\partial x} \right), \tag{2}$$

the strain compatibility equation

$$\frac{\partial^2 \varepsilon_{xx}}{\partial y^2} + \frac{\partial^2 \varepsilon_{yy}}{\partial x^2} = 2 \frac{\partial^2 \varepsilon_{xy}}{\partial x \partial y} \tag{3}$$

is satisfied identically for any  $u_x, u_y$  for which the respective third derivatives exist. Thus, it looks quite convenient to solve the problem first in displacements, and then to differentiate them to get the stresses from Hooke’s law, which takes, in the plane strain case, the form of:

$$\begin{pmatrix} \tau_{xx} \\ \tau_{yy} \\ \tau_{xy} \end{pmatrix} = \frac{E}{1+\nu} \begin{bmatrix} \frac{1-\nu}{1-2\nu} & \frac{\nu}{1-2\nu} & 0 \\ \frac{\nu}{1-2\nu} & \frac{1-\nu}{1-2\nu} & 0 \\ 0 & 0 & \frac{1}{2} \end{bmatrix} \begin{pmatrix} \varepsilon_{xx} \\ \varepsilon_{yy} \\ 2\varepsilon_{xy} \end{pmatrix}, \quad \text{or} \tag{4}$$

$$\begin{pmatrix} \tau_{xx} \\ \tau_{yy} \\ \tau_{xy} \end{pmatrix} = \begin{bmatrix} \lambda + 2\mu & \lambda & 0 \\ \lambda & \lambda + 2\mu & 0 \\ 0 & 0 & \mu \end{bmatrix} \begin{pmatrix} \varepsilon_{xx} \\ \varepsilon_{yy} \\ 2\varepsilon_{xy} \end{pmatrix},$$

where  $\lambda = \frac{\nu E}{(1-2\nu)(1+\nu)}$  and  $\mu = \frac{E}{2(1+\nu)}$  are Lamé constants.

Substituting (2) into (4) and subsequently the result into (1), we obtain for  $u_x, u_y$  the partial differential equations to be solved:

$$\left[ 2(1-\nu) \frac{\partial^2}{\partial x^2} + (1-2\nu) \frac{\partial^2}{\partial y^2} \right] u_x + \frac{\partial^2 u_y}{\partial x \partial y} = 0, \tag{5a}$$

$$\frac{\partial^2 u_x}{\partial x \partial y} + \left[ (1-2\nu) \frac{\partial^2}{\partial x^2} + 2(1-\nu) \frac{\partial^2}{\partial y^2} \right] u_y + \frac{2(1-2\nu)(1+\nu)\rho g}{E} = 0. \tag{5b}$$

In accordance with *Rekach (1977, p. 81)*, we will be looking for  $u_x, u_y$ , and  $\tau_{xx}, \tau_{yy}, \tau_{xy}$  in the form:

$$u_x = \frac{1}{1-\nu} \frac{\partial^2 \varphi}{\partial x \partial y}, \tag{6a}$$

$$u_y = -2 \frac{\partial^2 \varphi}{\partial x^2} - \frac{1 - 2\nu}{1 - \nu} \frac{\partial^2 \varphi}{\partial y^2}, \quad (6b)$$

$$\tau_{xx} = E \left( \frac{1}{1 + \nu} \frac{\partial^3 \varphi}{\partial x^2 \partial y} - \frac{\nu}{1 - \nu^2} \frac{\partial^3 \varphi}{\partial y^3} \right), \quad (6c)$$

$$\tau_{yy} = -E \left( \frac{2 - \nu}{1 - \nu^2} \frac{\partial^3 \varphi}{\partial x^2 \partial y} + \frac{1}{1 + \nu} \frac{\partial^3 \varphi}{\partial y^3} \right), \quad (6d)$$

$$\tau_{xy} = E \left( \frac{\nu}{1 - \nu^2} \frac{\partial^3 \varphi}{\partial x \partial y^2} - \frac{1}{1 + \nu} \frac{\partial^3 \varphi}{\partial x^3} \right), \quad (6e)$$

where  $\varphi$  is *not* the Airy *stress* function, but a function with a similar role with respect to the displacement.

With (6a,b), equation (5a) is satisfied identically. From (5b) we will get the biharmonic equation with non-zero right-hand side:

$$\frac{\partial^4 \varphi}{\partial x^4} + 2 \frac{\partial^4 \varphi}{\partial x^2 \partial y^2} + \frac{\partial^4 \varphi}{\partial y^4} = \frac{(1 + \nu) \rho g}{E} = \frac{\rho g}{2\mu}. \quad (7)$$

Let us compose  $\varphi$  traditionally of  $\varphi_0 + \varphi_g$  such that

$$\frac{\partial^4 \varphi_0}{\partial x^4} + 2 \frac{\partial^4 \varphi_0}{\partial x^2 \partial y^2} + \frac{\partial^4 \varphi_0}{\partial y^4} = 0, \quad (8a)$$

$$\frac{\partial^4 \varphi_g}{\partial x^4} + 2 \frac{\partial^4 \varphi_g}{\partial x^2 \partial y^2} + \frac{\partial^4 \varphi_g}{\partial y^4} = \frac{(1 + \nu) \rho g}{E}. \quad (8b)$$

The particular solution  $\varphi_g$  shall be chosen to satisfy identically, besides of (8b), only *some* of the boundary conditions, and *fail* – the more the better – to satisfy the remaining boundary conditions. The *difference* between the desired satisfaction of the latter boundary conditions by  $\varphi$  and the actual non-satisfaction of the same by  $\varphi_g$  will be input into the process of solving (8a) as the prescribed (nonzero) boundary conditions for  $\varphi_0$  – the *loading functions*. The homogeneous solution  $\varphi_0$  must be of course construed to satisfy identically a *subset* of the boundary conditions identically satisfied by  $\varphi_g$ .

In the sequel, we shall:

- denote displacements and stresses corresponding to the particular own-weight solution  $\varphi_g$  with an additional subscript “ $g$ ” for general or constant gravity and “*glin*” for linear gravity, e.g.  $u_{xg}, u_{yg}$ ,
- leave the displacements and stresses corresponding to homogeneous solution  $\varphi_0$  without any additional subscript, e.g.  $u_x, u_y$ ,
- add an extra subscript “ $t$ ” to denote the total displacements and stresses corresponding to the solution  $\varphi$ , e.g.  $u_{xt}, u_{yt}$ .

#### 4. The own weight

In the case of constant  $\rho g$ , we do not need to solve (8b) in order to find the loading functions. Instead, it is more efficient to guess directly the (polynomial) formulas for displacements or stresses, with some constants left to be determined after the substitution of such solutions into (1).

One can try to find an explicit formula of  $\varphi_g(y)$  for some  $(\rho g)(y)$  as well. In a solved and commented example problem in section 8, we will, for constant  $\rho$  and linear  $g(y)$ , find  $\varphi_{glin}$  polynomial in  $y$ . For arbitrary  $(\rho g)(x, y)$ , we cannot give a simple recipe, thus we will not treat this general case here.

In our small dimensions applications (tidal deformations at the site, seismometry of speleothems), the gravity  $g$  can be considered as spatially constant.

#### 5. The boundary conditions

We will here restrain ourselves to symmetrical problems, where  $\varphi$  is an even function of both  $x$  and  $y$ . It is advisable to choose an even  $\varphi_g$ . Then the homogeneous solution  $\varphi_0$  is even, too, and its general form (which differs from method to method) is simple and easy to handle. For a constant body force  $\rho g$ , symmetry of  $\varphi$  is achieved if the geometry of the domain, *and* of the boundary conditions, is symmetric. This requires to prescribe the same boundary conditions for the opposite sides of the rectangle. They are ready to be formulated after the substitution of the assumed general form of

$\varphi_0$  into the formulas (6a,b) for displacement boundary conditions, and into (6c,d,e) for stress boundary conditions. Due to the symmetry, it is enough to make use of the boundary conditions for the halves of the two adjacent sides.

Even though the *mixed* stress-displacement boundary problem is the one most often encountered in reality, we will select for our method contest a pure displacement boundary problem (zero displacements all around). The main reason is to have an interesting contest – with this setting, we will have a more narrow winner.

In the method of superposition, and in the method of homogeneous solutions, as  $\varphi_0$  satisfies the biharmonic equation identically for *any* values of the Fourier coefficients, the *only criterion* of the quality of the solution is the satisfaction of boundary conditions. Therefore, in section 10 we will construct plots showing the fulfillment of the *boundary conditions* all around the boundary calling them *boucograms*. They will be the strongest indicators of who the winner is.

## 6. Method of homogeneous solutions

A very compact and useful user instruction to this method can be found in *Rekach (1977, pp. 81-82)*. Where possible, we will use the same notation.

Let us choose the particular solution

$$\varphi_g = \frac{\rho g}{\mu} \left( \frac{y^4}{48} - \frac{b^2 y^2}{8} \right),$$

which satisfies

$$u_x(x, b) = -u_x(x, -b) = 0, \quad u_y(x, b) = u_y(x, -b) = 0,$$

and search for the approximate homogeneous solution of the boundary problem

$$u_x(x, b) = -u_x(x, -b) = 0, \quad u_y(x, b) = u_y(x, -b) = 0,$$

$$u_x(a, y) = -u_x(-a, y) = -u_x(a, y) = 0, \quad u_y(a, y) = u_y(-a, y) = -u_y(a, y),$$

in the form:

$$\varphi_0(x, y) = \sum_{n=1}^N (A_n \cosh k_n y + D_n y \sinh k_n y) \cos k_n x, \tag{9}$$

where  $k_n, A_n, D_n$  are constants to be determined. The assumed homogeneous solution (9) identically satisfies the homogeneous biharmonic equation (8a) and is even in  $x$  and  $y$ .

The respective displacements are:

$$u_x(x, y) = \frac{-1}{1 - \nu} \sum_{n=1}^N k_n \left[ (k_n A_n + D_n) \sinh k_n y + k_n D_n y \cosh k_n y \right] \sin k_n x \tag{10a}$$

$$u_y(x, y) = \frac{1}{1 - \nu} \sum_{n=1}^N k_n \left[ (k_n A_n - 2(1 - 2\nu) D_n) \cosh k_n y + k_n D_n y \sinh k_n y \right] \cos k_n x \tag{10b}$$

Let us formulate the boundary conditions to be satisfied identically:  $u_x(x, b) = -u_x(x, -b) = 0, u_y(x, b) = u_y(x, -b) = 0$ , denoting  $k_n b = \kappa_n$ :

$$\begin{Bmatrix} 0 \\ 0 \end{Bmatrix} = \begin{bmatrix} k_n \sinh \kappa_n \sin k_n x & (\kappa_n \cosh \kappa_n + \sinh \kappa_n) \sin k_n x \\ k_n \cosh \kappa_n \cos k_n x & (\kappa_n \sinh \kappa_n - 2(1 - 2\nu) \cosh \kappa_n) \cos k_n x \end{bmatrix} \begin{Bmatrix} A_n \\ D_n \end{Bmatrix}$$

We will get nonzero solution either for  $k_n = 0$  (corresponds to a needless constant term in  $\varphi_0$ ) or  $\kappa_n$  satisfying the characteristic equation

$$\det \begin{bmatrix} \sinh \kappa_n & \kappa_n \cosh \kappa_n + \sinh \kappa_n \\ \cosh \kappa_n & \kappa_n \sinh \kappa_n - 2(1 - 2\nu) \cosh \kappa_n \end{bmatrix} = 0,$$

which gives after some arrangement:

$$2\kappa_n = -(3 - 4\nu) \sinh 2\kappa_n. \tag{11a}$$

The corresponding solution is then:

$$D_n = -\frac{A_n k_n \sinh \kappa_n}{\kappa_n \cosh \kappa_n + \sinh \kappa_n}.$$



With the introduction of  $r_n = \text{Re } \kappa_n$ ,  $p_n = \text{Im } \kappa_n$ , the characteristic equation (11a) can be split into two equations for real and imaginary parts:

$$\frac{2r_n}{\sinh 2r_n} = -(3 - 4\nu) \cos 2p_n \quad \text{and} \quad \frac{2p_n}{\cosh 2r_n} = -(3 - 4\nu) \sin 2p_n, \quad (11b)$$

whence  $p_n$  can be eliminated:

$$p_n = \pm \frac{1}{2} \sqrt{(3 - 4\nu)^2 - \frac{4r_n^2}{\sinh^2 2r_n}} \cosh 2r_n, \quad (12a)$$

Besides of this equation, we have to, for the determination of  $r_n$ , keep both the equations (11b), i.e. after the elimination of  $p_n$ :

$$\frac{2r_n}{\sinh 2r_n} = -(3 - 4\nu) \cos \left( \sqrt{(3 - 4\nu)^2 - \frac{4r_n^2}{\sinh^2 2r_n}} \cosh 2r_n \right), \quad (12b)$$

$$\begin{aligned} \sqrt{(3 - 4\nu)^2 - \frac{4r_n^2}{\sinh^2 2r_n}} &= \\ &= -(3 - 4\nu) \sin \left( \sqrt{(3 - 4\nu)^2 - \frac{4r_n^2}{\sinh^2 2r_n}} \cosh 2r_n \right). \end{aligned} \quad (12c)$$

The reason becomes fully apparent by examining the graphs of (12b,c) in Fig. 2: Only even roots of (12b) (or odd roots of (12c)), marked by grey dots, correspond to the roots  $\kappa_n = r_n + jp_n$  of the characteristic equation (11a).

The roots of (12b) or (12c) can be found numerically. Of these two, it is more reliable to search for roots of (12b) and then to pick up every second one. We used for it the Mathematica 4 implementation of damped Newton's method with the default settings.

After the substitution of the solutions into (9) and (10) we have

$$\varphi_0(x, y) = \sum_{n=1}^N A_n \left( \cosh \frac{\kappa_n y}{b} - \frac{\kappa_n y}{b} \frac{\sinh \kappa_n \sinh \frac{\kappa_n y}{b}}{\kappa_n \cosh \kappa_n + \sinh \kappa_n} \right) \cos \frac{\kappa_n x}{b},$$

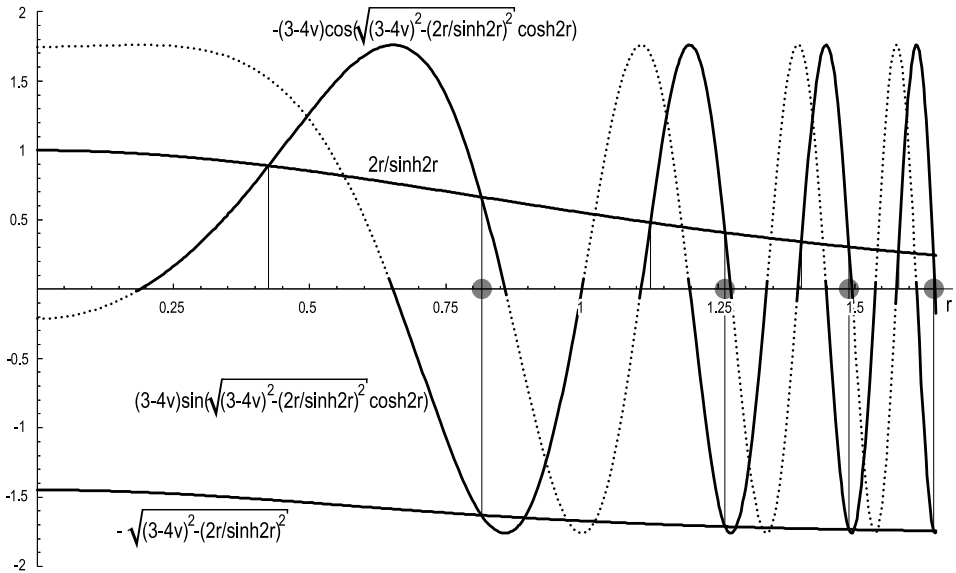


Fig. 2. Search for the real part of the roots of the characteristic equation for  $\nu = 0.31$  in the method of homogeneous solutions of the zero-displacement boundary problem.

and

$$u_x(x, y) = \frac{1}{1 - \nu} \sum_{n=1}^N A_n \frac{\kappa_n^2}{b^2} \left[ \frac{\frac{\kappa_n y}{b} \cosh \frac{\kappa_n y}{b} \sinh \kappa_n}{\kappa_n \cosh \kappa_n + \sinh \kappa_n} - \frac{\kappa_n \cosh \kappa_n \sinh \frac{\kappa_n y}{b}}{\kappa_n \cosh \kappa_n + \sinh \kappa_n} \right] \sin \frac{\kappa_n x}{b}, \quad (13a)$$

$$u_y(x, y) = \frac{1}{1 - \nu} \sum_{n=1}^N A_n \frac{\kappa_n^2}{b^2} \left[ \frac{\kappa_n \cosh \kappa_n \cosh \frac{\kappa_n y}{b}}{\kappa_n \cosh \kappa_n + \sinh \kappa_n} + \frac{\left( (3 - 4\nu) \cosh \frac{\kappa_n y}{b} - \frac{\kappa_n y}{b} \sinh \frac{\kappa_n y}{b} \right) \sinh \kappa_n}{\kappa_n \cosh \kappa_n + \sinh \kappa_n} \right] \cos \frac{\kappa_n x}{b}. \quad (13b)$$

Now the task is to find such values of coefficients  $A_n$ , that would achieve the best possible approximation to the fulfillment of the boundary conditions  $u_x(a, y) = -u_{xg}(a, y)$  and  $u_y(a, y) = -u_{yg}(a, y)$ . There are basically two approaches to it: either to take samples of  $-u_{xg}(a, y)$  and  $-u_{yg}(a, y)$  directly in spatial domain, as proposed in *Rekach (1977, pp. 81-82)*, or to expand  $u_x(a, y)$ ,  $u_y(a, y)$ ,  $-u_{xg}(a, y)$ ,  $-u_{yg}(a, y)$  into ordinary Fourier series, thus taking samples in the frequency domain.

In the case of direct sampling, one has to avoid taking samples of  $u_x(a, y)$  in, or very near, the points where  $u_x(a, y) = 0$  regardless of  $A_n$  – i.e., in the corner and in the midpoint of the side.

As for the sampling in frequency domain, the nature of the expected final solution (Fig. 3) suggests the expansion of  $u_x(a, y)$  and  $-u_{xg}(a, y)$  into series in  $\sin(l\pi y/b)$  and of  $u_y(a, y)$  and  $-u_{yg}(a, y)$  into series in  $\cos[(2m-1)\pi y/2b]$  ( $l, m$  are natural) as the best option. Paradoxically, as we will show in numerical results, the opposite (in arguments) is true!

## 7. Method of superposition

A well comprehensible explanation of this method can be found in *Meleshko (1995)*. In the application to our case we will closely adhere, with some exceptions in favour of the coherence of our paper, to his notation.

We will use the same particular own-weight solution  $\varphi_g$  with corresponding displacements  $u_{xg}$ ,  $u_{yg}$  as in the method of homogeneous solutions. Let us search for the homogeneous solution of the same boundary problem  $u_x(x, b) = -u_x(x, -b) = 0$ ,  $u_y(x, b) = u_y(x, -b) = 0$ ,  $u_x(a, y) = -u_x(-a, y) = -u_{xg}(a, y) = 0$ ,  $u_y(a, y) = u_y(-a, y) = -u_{yg}(a, y)$  in the form:

$$\begin{aligned} \varphi_0(x, y) = & -\frac{1-\nu}{2(1-2\nu)}C_0y^2 - \\ & - \sum_{n=1}^{\infty} \left( A_n \alpha_n x \frac{\sinh \alpha_n x}{\sinh \alpha_n a} + C_n \frac{\cosh \alpha_n x}{\sinh \alpha_n a} \right) \frac{\cos \alpha_n y}{\alpha_n^2} - \frac{D_0 x^2}{4} - \\ & - \sum_{m=1}^{\infty} \left( B_m \beta_m y \frac{\sinh \beta_m y}{\sinh \beta_m b} + D_m \frac{\cosh \beta_m y}{\sinh \beta_m b} \right) \frac{\cos \beta_m x}{\beta_m^2}, \end{aligned} \quad (14)$$

where  $\alpha_n = n\pi/b$ ,  $\beta_m = m\pi/a$ , and  $A_n, B_m, C_n, D_m$  are constants to be determined, which identically satisfies the homogeneous biharmonic equation (8a) and is even in  $x$  and  $y$ .

Let us denote  $-u_{yg}(a, y) = f(y)$ . For the chosen  $\varphi_g$ ,  $-u_{xg}(a, y) = 0$ . We shall expand  $f(y)$  into Fourier series

$$f(y) = f_0 + \sum_{n=1}^{\infty} (-1)^n f_n \cos \alpha_n y, \tag{15}$$

where

$$f_0 = \frac{1}{2b} \int_{-b}^b f(y) dy, \quad f_n = \frac{(-1)^n}{b} \int_{-b}^b f(y) \cos \alpha_n y dy, \tag{16}$$

The conditions to be satisfied identically:  $u_x(a, y) = -u_x(-a, y) = 0$ ,  $u_x(x, b) = -u_x(x, -b) = 0$  lead to

$$C_n = -A_n (1 + \alpha_n a \coth \alpha_n a), \quad D_m = -B_m (1 + \beta_m b \coth \beta_m b). \tag{17}$$

Then the boundary conditions for  $u_y(a, y)$ ,  $u_y(x, b)$  can be formulated:

$$\begin{aligned} u_y(a, y) = C_0 + D_0 + \frac{1}{1-\nu} \sum_{n=1}^{\infty} A_n \left( (3-4\nu) \coth \alpha_n a - \right. \\ \left. - \frac{\alpha_n a}{\sinh^2 \alpha_n a} \right) \cos \alpha_n y + \frac{1}{1-\nu} \sum_{m=1}^{\infty} B_m (-1)^m \times \\ \times \left( (3-4\nu + \beta_m b \coth \beta_m b) \frac{\cosh \beta_m y}{\sinh \beta_m b} - \beta_m y \frac{\sinh \beta_m y}{\sinh \beta_m b} \right) = f(y), \end{aligned} \tag{18a}$$

$$\begin{aligned} u_y(x, b) = C_0 + D_0 + \frac{1}{1-\nu} \sum_{m=1}^{\infty} B_m \left( (3-4\nu) \coth \beta_m b + \right. \\ \left. + \frac{\beta_m b}{\sinh^2 \beta_m b} \right) \cos \beta_m x + \frac{1}{1-\nu} \sum_{n=1}^{\infty} A_n (-1)^n \times \\ \times \left( (3-4\nu - \alpha_n a \coth \alpha_n a) \frac{\cosh \alpha_n x}{\sinh \alpha_n a} + \alpha_n x \frac{\sinh \alpha_n x}{\sinh \alpha_n a} \right) = 0. \end{aligned} \tag{18b}$$

Expanding the terms of the second sums in (18a), (18b) into Fourier series in  $\cos \alpha_n y$  and  $\cos \beta_m x$ , respectively, and after the substitution  $X_n = (-1)^n A_n \alpha_n / a$ ,  $Y_m = -(-1)^m B_m \beta_m / b$  we obtain:

$$C - 4 \sum_{m=1}^{\infty} Y_m / \beta_m^2 = f_0, \quad C + 2\sigma \sum_{n=1}^{\infty} X_n / \alpha_n^2 = 0, \tag{19}$$

and the infinite system of linear algebraic equations:

$$\frac{1}{1-\nu} X_n a^2 \Delta_a(\alpha_n a) = f_n + 4 \sum_{m=1}^{\infty} Y_m \frac{\sigma \alpha_n^2 + 2\beta_m^2}{(\alpha_n^2 + \beta_m^2)^2}, \tag{20a}$$

$$\frac{1}{1-\nu} Y_m b^2 \Delta_b(\beta_m b) = 4 \sum_{n=1}^{\infty} X_n \frac{\sigma \alpha_n^2 + 2\beta_m^2}{(\alpha_n^2 + \beta_m^2)^2}, \tag{20b}$$

where  $\sigma = \frac{1-2\nu}{1-\nu}$ ,  $C = C_0 + D_0$ ,  $\Delta_a(\alpha_n a) = \left( \frac{(3-4\nu) \coth \alpha_n a}{\alpha_n a} - \frac{1}{\sinh^2 \alpha_n a} \right)$  and  $\Delta_b(\beta_m b) = \left( \frac{(3-4\nu) \coth \beta_m b}{\beta_m b} + \frac{1}{\sinh^2 \beta_m b} \right)$ . This infinite system is regular (Meleshko and Gomilko, 1997, p. 2140, inequality 1.3), as:

$$\xi_n = 1 - \left| \frac{4}{a^2 \Delta_a(\alpha_n a)} \sum_{m=1}^{\infty} \frac{(1-2\nu) \alpha_n^2 + 2(1-\nu) \beta_m^2}{(\alpha_n^2 + \beta_m^2)^2} \right| = \frac{2-4\nu}{\alpha_n^2 a^2 \Delta_a(\alpha_n a)} > 0,$$

$$\eta_m = 1 - \left| \frac{4}{b^2 \Delta_b(\beta_m b)} \sum_{n=1}^{\infty} \frac{(1-2\nu) \alpha_n^2 + 2(1-\nu) \beta_m^2}{(\alpha_n^2 + \beta_m^2)^2} \right| = \frac{4-4\nu}{\beta_m^2 b^2 \Delta_b(\beta_m b)} > 0.$$

The coefficients of the expansion of

$$f(y) = \frac{\rho g (1+\nu) (1-2\nu) (y^2 - b^2)}{2(1-\nu) E}$$

into Fourier series in  $\cos \alpha_n y$ ,  $\alpha_n = n\pi/b$  are:

$$f_0 = -\frac{\rho g (1+\nu) (1-2\nu) b^2}{3(1-\nu) E} \quad \text{and} \quad f_n = \frac{2\rho g (1+\nu) (1-2\nu)}{\alpha_n^2 (1-\nu) E}.$$

The infinite system has a bounded solution, because, in the notation of (*ibid*, p. 2141, inequality 1.5):

$$|d_m| = 0 \quad \text{and} \quad |b_n| = \left| \frac{f_n (1-\nu)}{a^2 \Delta_a(\alpha_n a)} \right| = \frac{2\rho g (1+\nu) (1-2\nu)}{\alpha_n^2 a^2 \Delta_a(\alpha_n a) E},$$

and obviously, a constant  $K$  can be found such that  $|b_n| \leq K\xi_n$ . Notice that the threshold value of  $K = |b_n|/\xi_n = \rho g(1 + \nu)/E = \rho g/2\mu$  is equal to the constant on the right hand side of the solved biharmonic equation (7).

Since our problem meets the criteria, we can apply the method of reduction of the number of unknowns  $X_n, Y_m$  to finite  $N$  and  $M$ , respectively. More precisely, we will use the *improved* reduction approach (Meleshko, 1995, p. 216) based on the asymptotic behaviour of  $X_n, Y_m$  (Koialovich, 1930):

$$X_n = x_n + G, \quad Y_m = y_m + G, \tag{21}$$

where  $G$  is a nonzero constant and  $\lim_{n \rightarrow \infty} x_n = 0, \lim_{m \rightarrow \infty} y_m = 0$ . Substituting (21) into (19) and (20), we obtain:

$$\begin{aligned} f_0 &= C - 4 \sum_{m=1}^{\infty} y_m/\beta_m^2 - 4G \sum_{m=1}^{\infty} 1/\beta_m^2 = C - 4 \sum_{m=1}^{\infty} y_m/\beta_m^2 - 2Ga^2/3 \approx \\ &\approx C - 4 \sum_{m=1}^M y_m/\beta_m^2 - 2Ga^2/3 \end{aligned} \tag{22a}$$

$$\begin{aligned} 0 &= C + 2\sigma \sum_{n=1}^{\infty} x_n/\alpha_n^2 + 2\sigma G \sum_{n=1}^{\infty} 1/\alpha_n^2 = C + 2\sigma \sum_{n=1}^{\infty} x_n/\alpha_n^2 + \sigma Gb^2/3 \approx \\ &\approx C + 2\sigma \sum_{n=1}^N x_n/\alpha_n^2 + \sigma Gb^2/3, \end{aligned} \tag{22b}$$

and

$$\begin{aligned} f_n &= \frac{2\sigma G}{\alpha_n^2} + x_n \frac{a^2 \Delta_a(\alpha_n a)}{1 - \nu} - 4 \sum_{m=1}^{\infty} y_m \frac{\sigma \alpha_n^2 + 2\beta_m^2}{(\alpha_n^2 + \beta_m^2)^2} \approx \\ &\approx \frac{2\sigma G}{\alpha_n^2} + x_n \frac{a^2 \Delta_a(\alpha_n a)}{1 - \nu} - 4 \sum_{m=1}^M y_m \frac{\sigma \alpha_n^2 + 2\beta_m^2}{(\alpha_n^2 + \beta_m^2)^2}, \end{aligned} \tag{23a}$$

$$\begin{aligned} 0 &= \frac{4G}{\beta_m^2} + y_m \frac{b^2 \Delta_b(\beta_m b)}{1 - \nu} - 4 \sum_{n=1}^{\infty} x_n \frac{\sigma \alpha_n^2 + 2\beta_m^2}{(\alpha_n^2 + \beta_m^2)^2} \approx \\ &\approx \frac{4G}{\beta_m^2} + y_m \frac{b^2 \Delta_b(\beta_m b)}{1 - \nu} - 4 \sum_{n=1}^N x_n \frac{\sigma \alpha_n^2 + 2\beta_m^2}{(\alpha_n^2 + \beta_m^2)^2}. \end{aligned} \tag{23b}$$

To simplify the notation, we will return to the exact equality sign *without* altering the notation of the unknowns after the reduction to, e.g.,  $x_n^{(N,M)}$ ,  $y_m^{(N,M)}$ ,  $C^{(N,M)}$ ,  $G^{(N,M)}$ . We shall nevertheless keep in mind that for finite  $N$  and  $M$ , the coefficients of the reduced system are not equal to those of the unreduced.

If we sum up the unreduced equation (23a) through all  $n$  and the unreduced equation (23b) through all  $m$ , and then add together the resulting sums, we get:

$$\sum_{n=1}^{\infty} f_n = f(b) - f_0 = G(2a^2 + \sigma b^2)/3 + 2\sigma \sum_{n=1}^{\infty} x_n/\alpha_n^2 + 4 \sum_{m=1}^{\infty} y_m/\beta_m^2. \tag{24}$$

From equations (22a) and (22b), though, we obtain a *different* equation:

$$-f_0 = G(2a^2 + \sigma b^2)/3 + 2\sigma \sum_{n=1}^{\infty} x_n/\alpha_n^2 + 4 \sum_{m=1}^{\infty} y_m/\beta_m^2.$$

Fortunately, our  $f(b) = 0$ . Equation (24) provides a simple but useful estimate of the order of error of the  $y$ -displacement corresponding to the reduced solution  $u_y^{(N,M)}(a, b)$ , which is  $u_y^{(N,M)}(a, b) - f(b) \approx -\sum_{n=0}^N f_n$ . The actual error will differ from this estimate, as (24) does not keep its validity after the reduction.

Once we have the solution  $C, G, x_1, \dots, x_N, y_1, \dots, y_M$  of the reduced linear system (22, 23), we can substitute (17) and the coefficient relationships

$$A_n = (-1)^n(x_n + G)a/\alpha_n, \quad B_m = -(-1)^m(y_m + G)b/\beta_m,$$

where  $x_n = 0$  for  $n > N$  and  $y_m = 0$  for  $m > M$ , into  $\varphi_0(x, y)$  (14) to yield:

$$\begin{aligned} \varphi_0(x, y) = & -\frac{C_0 y^2}{2\sigma} - \frac{(C - C_0) x^2}{4} - \\ & - a \sum_{n=1}^N (-1)^n x_n \left( \frac{x \sinh \alpha_n x}{\sinh \alpha_n a} - \left( \frac{1}{\alpha_n} + a \coth \alpha_n a \right) \frac{\cosh \alpha_n x}{\sinh \alpha_n a} \right) \frac{\cos \alpha_n y}{\alpha_n^2} + \\ & + b \sum_{m=1}^M (-1)^m y_m \left( \frac{y \sinh \beta_m y}{\sinh \beta_m b} - \left( \frac{1}{\beta_m} + b \coth \beta_m b \right) \frac{\cosh \beta_m y}{\sinh \beta_m b} \right) \frac{\cos \beta_m x}{\beta_m^2} + \\ & + G \left( \frac{b^4 - a^4}{45} + \frac{(a^2 - x^2)^2 - (b^2 - y^2)^2}{24} \right), \end{aligned}$$

because, according to *Meleshko (1997, p. 33)*:

$$\begin{aligned}
 & -Ga \sum_{n=1}^{\infty} (-1)^n \left( \frac{x \sinh \alpha_n x}{\sinh \alpha_n a} - \left( \frac{1}{\alpha_n} + a \coth \alpha_n a \right) \frac{\cosh \alpha_n x}{\sinh \alpha_n a} \right) \frac{\cos \alpha_n y}{\alpha_n^2} + \\
 & +Gb \sum_{m=1}^{\infty} (-1)^m \left( \frac{y \sinh \beta_m y}{\sinh \beta_m b} - \left( \frac{1}{\beta_m} + b \coth \beta_m b \right) \frac{\cosh \beta_m y}{\sinh \beta_m b} \right) \frac{\cos \beta_m x}{\beta_m^2} = \\
 & = G \left( \frac{b^4 - a^4}{45} + \frac{(a^2 - x^2)^2 - (b^2 - y^2)^2}{24} \right).
 \end{aligned}$$

The value of  $C_0$  can be chosen freely. We leave the derivation of displacements and stresses to the reader.

Here, one may dislike the slow decrease of  $f_n$  with  $n$ , responsible for the corner error of  $u_y$  and for the ‘narrow’ (i.e. within the same order) fulfillment of the bounded solution criterion with its slightly unpleasant numerical implications, but there is not too much to do with it, save of finding a better particular solution or using – from the very beginning – another trigonometric system for Fourier expansion. Why do we put stress on the very beginning? We tried to expand (18a) and (18b), the terms with  $\cos \alpha_n y$ ,  $\cos \beta_m x$  as well, into the series in  $\cos \gamma_l y$ ,  $\cos \delta_k x$  with  $\gamma_l = (2l-1)\pi/2b$ ,  $\delta_k = (2k-1)\pi/2a$ . It worked, but the error of this solution near the corner was greater than with the standard expansion. If one wants to use the series in  $\cos \gamma_l y$ ,  $\cos \delta_k x$ , (s)he has to do so not later than in formulating the boundary conditions to be satisfied identically  $u_y(a, y) = u_y(-a, y) = 0$ ,  $u_y(x, b) = u_y(x, -b) = 0$  for eliminating half of the unknown coefficients (corresponds to the stage (17) here). These boundary conditions require taking another particular solution:

$$\varphi_g = \frac{\rho g}{\mu} \left( \frac{(1 - 2\nu)^2 x^4}{48} + \frac{(1 - \nu)^2 y^4}{12} - \frac{(1 - \nu)(1 - 2\nu)x^2 y^2}{4} \right),$$

for instance. With series in  $\cos \gamma_l y$ ,  $\cos \delta_k x$ , one has to take into account another asymptotic behaviour of the unknowns (*Meleshko and Gomilko, 1997, p. 2146, eq. 2.28*). At the end, one should arrive at  $u_y$  perfectly fulfilling the boundary conditions and  $u_x$  oscillating at the boundaries – the opposite to the solution presented here.



### 8. Choose your own weight!

After we have, in previous sections, realized the interdependence of the choice of the particular solution  $\varphi_g$  and of the choice of boundary conditions to be satisfied identically, we are able, for constant body force  $\rho g$ , to fill in the following overview table (Tab. 1):

Tab. 1. Overview of own-weight particular solutions corresponding to combinations of boundary conditions

	$u_x(x, b) = 0$	$u_y(x, b) = 0$	$u_y(a, y) = 0$
$u_x(a, y) = 0$	superposition $\varphi_g = \frac{\rho g}{\mu} \left( \frac{y^4}{48} - \frac{b^2 y^2}{8} \right)$ or $\varphi_g = \frac{\rho g}{\mu} \left( \frac{x^4}{48} - \frac{a^2 x^2}{8} \right)$	superposition $\varphi_g = \frac{\rho g}{\mu} \left( \frac{y^4}{48} - \frac{b^2 y^2}{8} \right)$	homogeneous solutions $\varphi_g = \frac{\rho g}{\mu} \left( \frac{x^4}{48} - \frac{a^2 x^2}{8} \right)$
$u_y(a, y) = 0$	superposition $\varphi_g = \frac{\rho g}{\mu} \left( \frac{x^4}{48} - \frac{a^2 x^2}{8} \right)$	superposition $\varphi_g = \frac{\rho g}{\mu} \left( \frac{(1-2\nu)^2 x^4}{48} + \frac{(1-\nu)^2 y^4}{12} - \frac{(1-\nu)(1-2\nu)x^2 y^2}{4} \right)$	
$u_y(x, b) = 0$	homogeneous solutions $\varphi_g = \frac{\rho g}{\mu} \left( \frac{y^4}{48} - \frac{b^2 y^2}{8} \right)$		

This table *suggests* the most appropriate method and the simplest polynomial particular solution to be used for the respective combination of boundary conditions (thick lines for easier orientation) to be satisfied identically.

In grey fields are the cases further investigated in this paper. We see that of all the six possible boundary conditions couples, the method of superposition can cover twice as many as the method of homogeneous solutions.

**Problem:** For the boundary conditions  $u_x(x, b) = 0, u_y(x, b) = 0$ , find the particular solution of the own weight problem in the case of constant  $\rho$  and linearly decreasing  $g = g_0 (1 - (h + y) / R)$ , where  $g_0$  is the gravity at the Earth’s surface,  $R$  is the radius of the Earth and  $h$  is the depth from the surface to the centerline of the very long rectangular parallelepiped whose length and upper and lower faces are parallel to the Earth’s surface (Fig. 1).

**Comment 1.:** An application instance could be a few km thick and wide (and much longer) subsurface deposit of a weak and very pure (constant  $\rho$ ) polycrystalline mineral in a much stiffer rock. The reader may either excuse the unrealistic features and oversimplifications involved here or forget about application and treat the problem as formally as it is stated.

**Solution:** If we, in the case of constant  $\rho g$ , substitute  $\varphi_g = \frac{\rho g}{\mu} \left( \frac{y^4}{48} - \frac{b^2 y^2}{8} \right)$  into (6a,b), we get  $u_{xg} = 0, u_{yg} = \frac{\rho g (b^2 - y^2)}{2\lambda + 4\mu}$  which satisfies the boundary conditions  $u_x(x, b) = -u_x(x, -b) = 0, u_y(x, b) = u_y(x, -b) = 0$ . We need to keep the term  $b^2 - y^2$  in the  $u_{yglin}$  corresponding to the solution  $\varphi_{glin}$  of our linear gravity problem, as well. It is reasonable to expect that  $\varphi_{glin}$  will be independent of  $x$ , and that  $u_{yglin}$  will include, compared to  $u_{yg}$ , an extra term. Let us therefore assume  $u_{xglin} = 0$  and  $u_{yglin} = \frac{\rho (b^2 - y^2)}{2\lambda + 4\mu} g(y)P(y)$ , the latter equivalent to  $\frac{\partial^2 \varphi_{glin}}{\partial y^2} = \frac{\rho (y^2 - b^2)}{4\mu} g(y)P(y)$ . With these assumptions, the biharmonic equation reduces to ordinary differential equation

$$\frac{\partial^4 \varphi_{glin}}{\partial y^4} = \frac{\rho g(y)}{2\mu},$$

written in full:

$$\rho \frac{(4yg' + (y^2 - b^2)g'') P + 2(y^2 - b^2)g'P' + (2P + 4yP' + (y^2 - b^2)P'') g}{4\mu} = \frac{\rho g}{2\mu},$$

whence after substitution of  $g = g_0 (1 - (h + y) / R)$  we get the equation for  $P(y)$ :

$$-2(R - h - y) + (R - h - 3y) P + 2((2R - 2h - 3y) y + b^2) P' + (y^2 - b^2) (R - h - y) P'' = 0.$$

The solution of this ODE is

$$P(y) = \frac{3Ry^2 - 3hy^2 - y^3 - 3C_1 - 3yC_2}{3(R - h - y)(y^2 - b^2)}.$$

In  $P(y)$ , the term  $(y^2 - b^2)$  in the denominator is not welcome at all. Therefore, the constants  $C_1, C_2$  must be chosen so that the term  $(y^2 - b^2)$  will appear in the numerator as well. In other words, if we denote the numerator of  $P(y)$  as  $N_P(y)$ , then  $N_P(b)$  and  $N_P(-b)$  must be zero. From these conditions, we determine  $C_1$  and  $C_2$  and get the final solution:

$$P(y) = \frac{3R - 3h - y}{3(R - h - y)}, \quad \varphi_{glin} = \frac{\rho g_0 (-3y^5 + 15(R - h)y^4 + 10b^2y^3 - 90(R - h)b^2y^2)}{720\mu R}.$$

**Comment 2.:** The found  $\varphi_{glin}$  is polynomial in  $y$ , and we are happy to see that for  $|y| < h \ll R$   $\varphi_{glin} = \varphi_g$ . Should we further solve this problem either by the method of homogeneous solutions or by superposition, the  $\varphi_{glin}$  would have to be separated into even and odd parts. For each of them, the respective  $\varphi_0$  can be constructed. The final  $\varphi$  would have to be recomposed of the even and odd particular and homogeneous solutions.

## 9. First look at the solution for constant own weight

In this section we present rough sketches of the results of numerical computations for  $a = 2$  m,  $b = 1$  m, a constant  $g = 9.81 \text{ m s}^{-2}$ ,  $\rho = 2712 \text{ kg m}^{-3}$ ,  $E = 8.38 \cdot 10^{10} \text{ Pa}$ ,  $\nu = 0.31$ . In the sequel, all other computation results will be given for the same values.

The purpose is to give us just an idea about how the solution looks like. A close look will follow in the next section. With proper implementation and enough terms in the Fourier expansions, the differences between the whole region plots of the results of the two methods – homogeneous solutions and superposition – are almost invisible to the naked eye.

The maximum tangential stress  $\tau_{\max t}$  in Fig. 3f was computed as  $\tau_{\max t} = \sqrt{\tau_{xyt}^2 + (\tau_{xxt} - \tau_{yyt})^2} / 4$ . The maximal absolute value of  $u_{xt}$  is  $u_{xt \max} = 1.306 \cdot 10^{-8}$  m reached at approximately  $[\pm 0.774 a, \pm 0.636 b]$  (Fig. 3a), the maximum of  $u_{yt}$  is  $u_{yt \max} = 1.173 \cdot 10^{-7}$  m reached at  $[0, 0]$  (Fig. 3b).

## 10. Close look at the solutions

Now it is time to use our microscope – the plot of the fulfillment of boundary conditions, or shortly, boucogram. The Fig. 4 explains how it is constructed.

Let us measure the length  $c$  of the anticlockwise ( $c \geq 0$ ) and clockwise ( $c < 0$ ) path around the boundary, starting in the point  $[0, b]$ . The boucograms of  $u_{xt}$  and  $u_{yt}$  are the plots of  $u_{xt}(c)_{achieved} - u_{xt}(c)_{prescribed} = u_{xt}(c) - 0$ ,  $u_{yt}(c)_{achieved} - u_{yt}(c)_{prescribed} = u_{yt}(c) - 0$ , respectively. The whole boundary is covered by  $c \in \langle -2a - 2b, 2a + 2b \rangle$ . Because of the symmetry ( $u_{xt}(c)$  and  $u_{xt}(c - 2a - 2b)$  are odd,  $u_{yt}(c)$  and  $u_{yt}(c - 2a - 2b)$  even), one gets the full information from boucograms on the interval  $\langle 0, a + b \rangle$  (triple line).

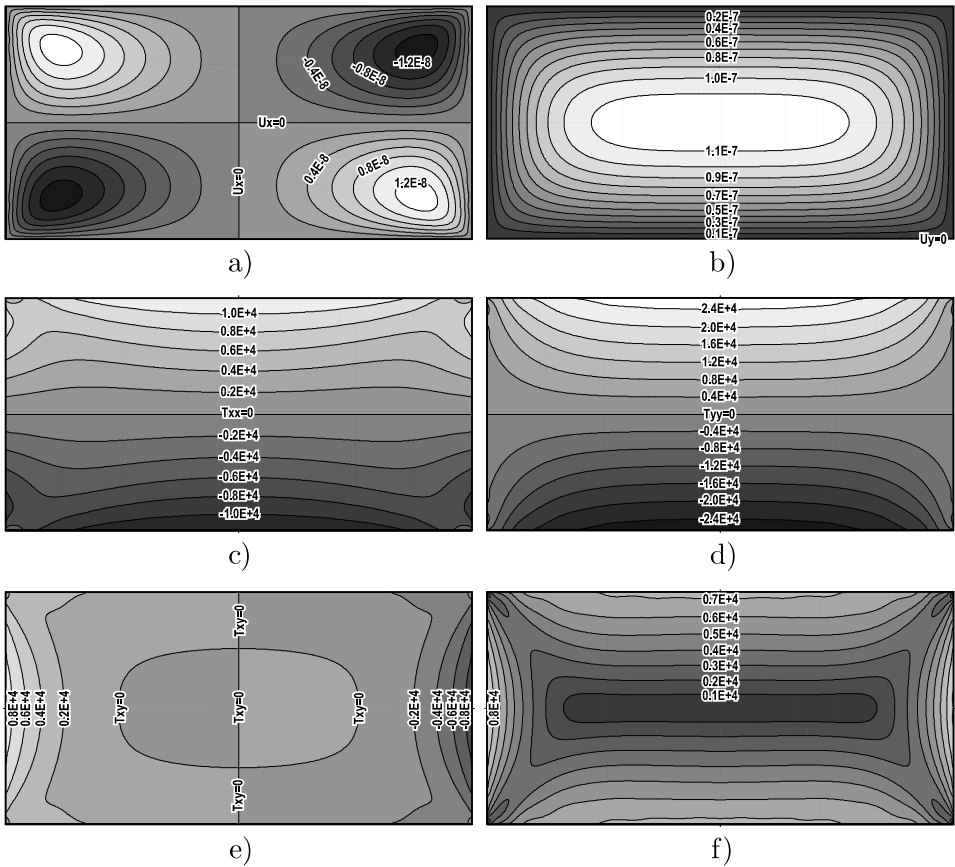


Fig. 3. Total displacement and stress fields in the elastic rectangle under own weight with zero-displacement fixation at the boundary; a) displacement  $u_{xt}$  [m] b) displacement  $u_{yt}$  [m] c) stress  $\tau_{xxx}$  [Pa] d) stress  $\tau_{yyy}$  [Pa] e) stress  $\tau_{xyt}$  [Pa] f) maximum tangential stress  $\tau_{max t}$  [Pa].

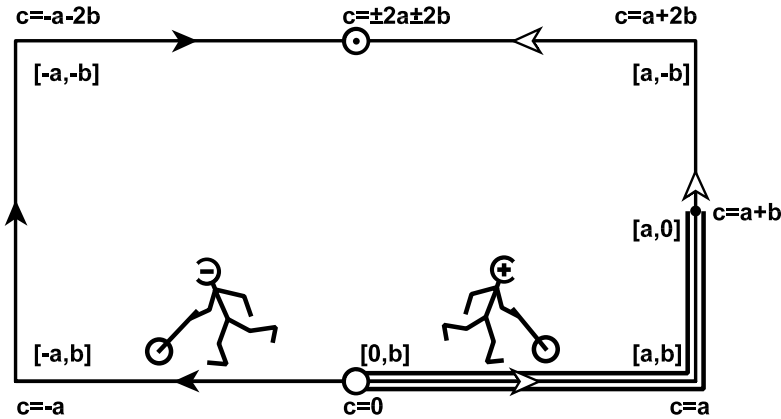


Fig. 4. Construction of a boucogram.

Fig. 5 shows the whole boundary boucograms  $u_{xt}(c)$ ,  $u_{yt}(c)$  (upper part) and their zoomed sections (lower part) for the own weight problem with  $\varphi_g = \frac{\rho g}{\mu} \left( \frac{y^4}{48} - \frac{b^2 y^2}{8} \right)$  solved by the method of homogeneous solution with identical satisfaction of  $u_x(x, b) = 0$ ,  $u_y(x, b) = 0$ . The remaining boundary conditions are covered by the first 10 and 10 frequency domain samples i.e. coefficients of the Fourier series of  $u_x(a, y)$  and of  $u_y(a, y)$ , respectively. Expansion of  $u_x(a, y)$  into  $\sin(l\pi y/b)$  and of  $u_y(a, y)$  into  $\cos[(2m - 1)\pi y/2b]$  was used, thus in both of these series, the zero frequency terms of all the functions involved are equal to zero.

Besides of the error signals  $u_{xt}(c)$ ,  $u_{yt}(c)$  themselves, their root mean squares are shown by white flat lines. They, together with the total misdisplacement  $u_t(c) = \sqrt{u_{xt}^2(c) + u_{yt}^2(c)}$  (black flat lines) are important indicators of the quality of the solution.

Fig. 6 shows the boucograms for the own weight problem, using the same  $\varphi_g$  as in previous example, solved by the method of superposition with identical satisfaction of  $u_x(a, y) = 0$ ,  $u_x(x, b) = 0$ . Again, altogether 20 samples were taken. In the expansions into  $\cos \alpha_n y$ ,  $\alpha_n = n\pi/b$  and  $\cos \beta_m x$ ,  $\beta_m = m\pi/a$ , one gets nonzero terms at zero frequencies, which definitely have to be involved in the computations, otherwise the baselines will drift away from the prescribed zero displacement. Thanks to the asymptotic behaviour of the unknowns, one can try to take advantage of the ‘infinite’

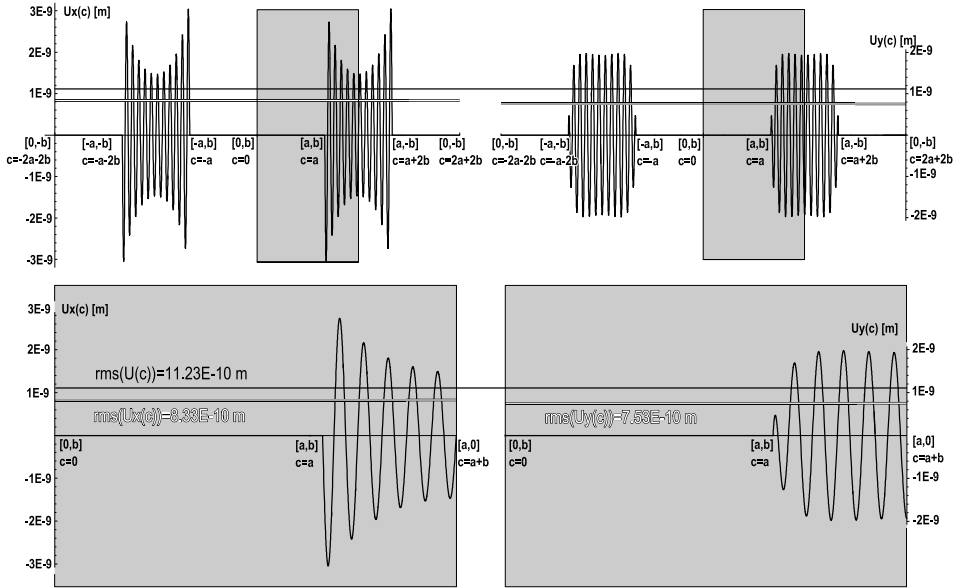


Fig. 5. Boucograms for own-weight, zero-displacement-boundary problem solved by method of homogeneous solutions.

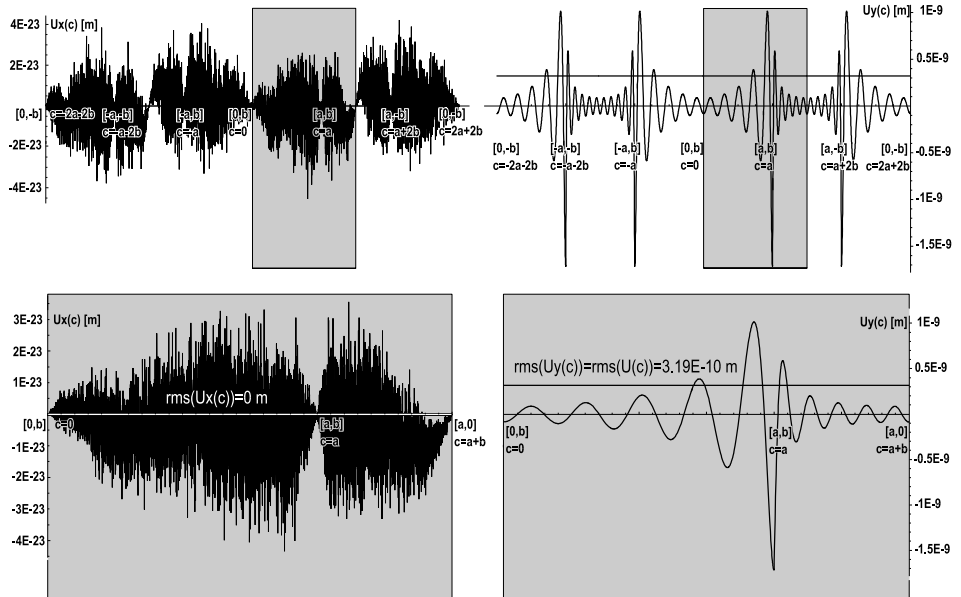


Fig. 6. Boucograms for own-weight, zero-displacement-boundary problem solved by the method of superposition.

frequencies samples (see 23a, 23b):

$$f_n \approx \frac{2\sigma G}{\alpha_n^2} - 4 \sum_{m=1}^M y_m \frac{\sigma \alpha_n^2 + 2\beta_m^2}{(\alpha_n^2 + \beta_m^2)^2} \quad \text{for } n \gg N \quad \text{and}$$

$$0 \approx \frac{4G}{\beta_m^2} - 4 \sum_{n=1}^N x_n \frac{\sigma \alpha_n^2 + 2\beta_m^2}{(\alpha_n^2 + \beta_m^2)^2} \quad \text{for } m \gg M.$$

The boucograms correspond to 1+9 samples taken of  $u_y(a, y) = f(y)$ : 1 zero frequency sample and 9 ‘ordinary’ frequencies samples for  $1 \leq n \leq 9$ , and 1+8+1 samples taken of  $u_y(x, b) = 0$ : 1 zero frequency sample, 8 samples for  $1 \leq m \leq 8$  and one ‘infinite’ frequency sample at  $m = 9 \cdot (10^6 + 1)$ . From thus constructed linear system, 9+9 coefficients  $x_n, y_m$ , for  $1 \leq n \leq 9, 1 \leq m \leq 9$  and 1+1 unknown constants  $C, G$  can be determined.

The ‘numerical noise’ in  $u_{xt}(c)$ , where the boundary conditions should be satisfied identically (17), is odd, too. We have plotted it in Fig. 6 just for completeness. In the overview of numerical results of the method of superposition, we will omit the plots  $u_{xt}(c)$  completely.

In  $u_{yt}(c)$ , a fact worth noticing is that  $|u_{yt}(c)|$  reaches its maximum value  $1.72 \cdot 10^{-9}$  m in the corners ( $u_{yt}(a, b) = -1.72 \cdot 10^{-9}$  m). The estimated error value according to (24) is, however,  $u_{yte}(a, b) = f(b) = -4.89 \cdot 10^{-9}$  m.

### 11. Overview of numerical results

The method of homogeneous solutions,  $\varphi_g = \frac{\rho g}{\mu} \left( \frac{y^4}{48} - \frac{b^2 y^2}{8} \right)$ , identical satisfaction of  $u_x(x, b) = 0, u_y(x, b) = 0$ : The total number of samples (identical with the number of unknown coefficients  $A_n$ ) is 20 (the most examples), 40 or 60 – the respective fields of the table are separated by thick lines. In Tab. 2 and 3, the relative displacement values are related to the displacement maxima given in section 9.

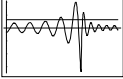
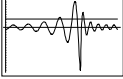
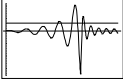
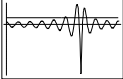
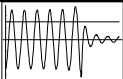
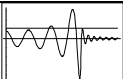
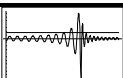
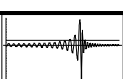
The method of superposition,  $\varphi_g = \frac{\rho g}{\mu} \left( \frac{y^4}{48} - \frac{b^2 y^2}{8} \right)$ , identical satisfaction of  $u_x(a, y) = 0, u_x(x, b) = 0$ : From totally  $N + M + 2$  samples, we have to determine  $N + M$  coefficients  $x_n, y_m$  and two constants  $C, G$ . The numbers  $N', M'$  of nonzero-frequencies coefficients of Fourier expansions of loading functions, stated in the respective columns of the table, do not need to be equal to  $N, M$ . They must be though  $N' \leq N, M' \leq M$ . In the columns

Tab. 2. Numerical results of the method of homogeneous solutions for various ways of sampling

sampling		boucograms	(relative) extremes of		(relative) rms of				
$u_x(a, y)$	$u_y(a, y)$	$u_x(c)$ $u_y(c)$	$u_x(c)$ [m]	at	$u_y(c)$ [m]	at	$u_x(c)$ [m]	$u_y(c)$ [m]	$u_l(c)$ [m]
direct linear $L = 10$ samples at $y = \frac{2l-1}{2L}b$ , $1 \leq l \leq L$	direct linear $M = 10$ samples at $y = \frac{2m-1}{2M}b$ , $1 \leq m \leq M$		1.08E-9 (0.083 $u_{y\max}$ )	[a, 0.5b]	-1.16E-9 (-0.0099 $u_{y\max}$ )	[a, 0]	3.03E-10 (0.023 $u_{y\max}$ )	3.33E-10 (0.0028 $u_{y\max}$ )	4.50E-10
sine Fourier $L = 10$ samples at $\omega_l = \frac{l\pi}{b}$ $1 \leq l \leq L$	cosine Fourier $M = 10$ samples at $\omega_m = \frac{(2m-1)\pi}{2b}$ $1 \leq m \leq M$		-3.04E-9 (-0.233 $u_{y\max}$ )	[a, 0.958b]	-1.98E-9 (-0.017 $u_{y\max}$ )	[a, 0.566b]	8.33E-10 (0.064 $u_{y\max}$ )	7.53E-10 (0.0064 $u_{y\max}$ )	11.23E-10
sine Fourier $L = 10$ samples at $\omega_l = \frac{(2l-1)\pi}{2b}$ $1 \leq l \leq L$	cosine Fourier $M = 10$ samples at $\omega_m = \frac{(2m-1)\pi}{2b}$ $1 \leq m \leq M$		-5.82E-10 (-0.044 $u_{y\max}$ )	[a, 0.905b]	8.18E-10 (0.0070 $u_{y\max}$ )	[a, 0.962b]	1.73E-10 (0.013 $u_{y\max}$ )	1.98E-10 (0.0017 $u_{y\max}$ )	2.63E-10
sine Fourier $L = 11$ samples at $\omega_l = \frac{l\pi}{b}$ $1 \leq l \leq L$	cosine Fourier $M+1=9$ samples at $\omega_m = \frac{m\pi}{b}$ $0 \leq m \leq M$		8.47E-10 (0.065 $u_{y\max}$ )	[a, 0.974b]	-8.55E-10 (-0.0072 $u_{y\max}$ )	[a, 0.883b]	1.55E-10 (0.0096 $u_{y\max}$ )	2.58E-10 (0.0022 $u_{y\max}$ )	2.87E-10
sine Fourier $L = 11$ samples at $\omega_l = \frac{(2l-1)\pi}{2b}$ $1 \leq l \leq L$	cosine Fourier $M+1=9$ samples at $\omega_m = \frac{m\pi}{b}$ $0 \leq m \leq M$		-4.69E-10 (-0.036 $u_{y\max}$ )	[a, 0.917b]	-7.73E-10 (-0.0066 $u_{y\max}$ )	[a, 0.889b]	1.16E-10 (0.0089 $u_{y\max}$ )	2.18E-10 (0.0019 $u_{y\max}$ )	2.47E-10
sine Fourier $L = 21$ samples at $\omega_l = \frac{(2l-1)\pi}{2b}$ $1 \leq l \leq L$	cosine Fourier $M+1=19$ samps at $\omega_m = \frac{m\pi}{b}$ $0 \leq m \leq M$		-4.13E-10 (-0.032 $u_{y\max}$ )	[a, 0.952b]	-5.11E-10 (-0.0044 $u_{y\max}$ )	[a, 0.846b]	1.04E-10 (0.0080 $u_{y\max}$ )	1.32E-10 (0.0011 $u_{y\max}$ )	1.68E-10
sine Fourier $L = 31$ samples at $\omega_l = \frac{(2l-1)\pi}{2b}$ $1 \leq l \leq L$	cosine Fourier $M+1= 29$ samps at $\omega_m = \frac{m\pi}{b}$ $0 \leq m \leq M$		-9.37E-10 (-0.072 $u_{y\max}$ )	[a, 0.905b]	-11.07E-10 (-0.0094 $u_{y\max}$ )	[a, 0.830b]	2.57E-10 (0.020 $u_{y\max}$ )	2.88E-10 (0.0025 $u_{y\max}$ )	3.86E-10



Tab. 3. Numerical results of the method of superposition for various ways of sampling

sampling						boucogram	(relative) extreme of		(relative) rms
$u_y(x,b)$			$u_y(a,y)$			$u_{yt}(c)$	$u_{yt}(c)$ [m]	at	$u_{yt}(c) = u_y(c)$ [m]
0	$M'$ $M$	$m_x$	0	$N'$ $N$	$n_x$				
1	9 9	-	1	9 9	-		-1.69E-9 (-0.014 $u_{jmax}$ )	[a,b]	3.19E-10 (0.0027 $u_{jmax}$ )
1	8 9	9(1E6+1)	1	9 9	-		-1.72E-9 (-0.015 $u_{jmax}$ )	[a,b]	3.19E-10 (0.0027 $u_{jmax}$ )
1	8 9	99	1	9 9	-		-1.74E-9 (-0.015 $u_{jmax}$ )	[a,b]	3.29E-10 (0.0028 $u_{jmax}$ )
1	12 12	-	1	6 6	-		-2.04E-9 (-0.017 $u_{jmax}$ )	[a,b]	2.86E-10 (0.0024 $u_{jmax}$ )
1	11 12	9(1E6+1)	1	6 6	-		-3.18E-9 (-0.027 $u_{jmax}$ )	[a,b]	1.50E-9 (0.013 $u_{jmax}$ )
1	6 6	-	1	12 12	-		-2.18E-9 (-0.019 $u_{jmax}$ )	[.988a,b]	5.62E-10 (0.0048 $u_{jmax}$ )
1	19 19	-	1	19 19	-		-6.14E-10 (-0.0052 $u_{jmax}$ )	[a,b]	8.07E-11 (0.0007 $u_{jmax}$ )
1	29 29	-	1	29 29	-		-3.42E-10 (-0.0029 $u_{jmax}$ )	[a,b]	3.65E-11 (0.0003 $u_{jmax}$ )

“0”, the *numbers* of samples at the respective zero frequencies are given. In the columns  $n_\infty$ ,  $m_\infty$  are the *values* of  $n_\infty \gg N$ ,  $m_\infty \gg M$ . No sample taken at ‘infinite’ frequency is indicated by “-”. More than one value of  $m_\infty$  (or  $n_\infty$ ) are conceivable as well (thus generated equations are still linearly independent), but the results are too disappointing to be stated here. Again, the table is subdivided into portions corresponding to 20, 40 and 60 samples by thick lines.

## 12. Who is the winner?

To make the answer easier, we have set up categories according to the number of samples. In the 20 samples category, we do have a surprise – the lowest values of all error indicators were attained by one of the implementations of the method of homogeneous solutions – see the gray fields in the Tab. 2. Here, the method of homogeneous solutions made the best of its home ground – it benefited from the identical satisfaction of boundary conditions on the longer sides and of investing all the available number of samples into dense coverage of the shorter sides.

In the 40 samples duel (forelast rows of the two tables), the superposition is already better in rms, but still defeated in maximum error. So, here we have a draw.

At 60 samples (last rows), the more sophisticated superposition method clearly shows its supremacy over the little bit brute homogeneous solutions, where (in our numerical implementation) the indicators are worse than at 40 samples!

The nice feature of the method of homogeneous solutions is that the satisfaction of the characteristic equation secures the zero displacements in the corners, whereas with the method of superposition, we get in the corners the error maxima of  $u_y$ . However, in the superposition method, we can find (rough) upper bound estimate of this corner error in advance – in the homogeneous solutions, to know the maximum error, we have to wait for the numerical solution. Other advantage of the method of superposition was already stated in the comment to the Tab. 1 – the superposition is “twice as universal” as the homogeneous solutions. Indeed, there can be practical situations where we have to insist on exact fulfillment of two of

the boundary conditions and can let the other two boundary conditions be fulfilled approximately. It is then more likely to find the right method among the superpositions.

### 13. Final comments on numerical results

In all cases, the values of coefficients of the Fourier series were computed directly from the respective linear systems by Gaussian elimination as implemented in `LinearSolve[]` in Mathematica 4.

In the method of homogeneous solutions (Tab. 2), all the sampling modes produced, according to the warnings issued by Mathematica, ill-conditioned matrices. Nevertheless, the solutions found can be considered as satisfactory. Notice that the direct linear sampling with its results is not completely lost among the frequency domain sampling modes. On the other hand, disappointing is the bad performance of the “best fit” expansions of  $u_x(a, y)$ ,  $u_y(a, y)$  into series in  $\sin(l\pi y/b)$  and  $\cos[(2m - 1)\pi y/2b]$ , respectively. Why are the “worst fit” expansions into  $\sin((2l - 1)\pi y/2b)$  and  $\cos[m\pi y/b]$  better? In our opinion, having in mind the way the Fourier coefficients are computed, the “worst fit” expansions, unlike the “best fit”, *emphasize the behaviour* of the expanded functions *near the corner* and thus provide valuable information for finding better-fitting coefficients.

In the method of superposition (Tab. 3), we immediately see something wrong with the numerical example in the fifth row. Indeed, it is a manifestation of a typical unsuccessful coefficient computation. Whereas in successful computations, the coefficients generally obey the asymptotic rule i.e. decrease with increasing index, here the coefficient  $y_{12}$  is more than ten times bigger than  $y_{11}$ . The coefficients  $x_n$  remained undisturbed, as can be seen in the right part of the boucogram as well. The ill-behaving  $y_{12}$  signals that the system does not like including the sample at  $m_\infty$ . This was the case for all the systems with unequal numbers  $N, M$  of coefficients  $x_n, y_m$ . It may look like that even in the cases, where  $m_\infty$  works ( $N = M$ ), it is not very helpful. Well, the quality indicators in the second and third row are slightly worse than in the first (without  $m_\infty$ ), but some positive effect, namely suppression of the ondulation in the middle of the longer side, is

clearly visible. Of course, objection can be raised, that if rms is approximately the same, then the ondulation there is lower *at the expense* of higher ondulation elsewhere. We think that adding a *little bit* to the error values that are big anyway is not an unbearable injustice. In neither of our numerical experiments were we successful with including the sample at  $n_\infty$ . In the 20 samples category, the *lowest rms* of error displacement was attained for the equal step sampling ( $N = 6$ ,  $M = 12$  – fourth row). The sixth row demonstrates that increasing the number of coefficients  $N$  to 12 did not help to lower the corner error, as would the equation (24) suggest.

## 14. Conclusions

To each of the six boundary condition couples, we have attributed one of the two Fourier methods and at least one of the three kinds of simple polynomial particular own-weight solutions (see Tab. 1). So, we found basically seven different ways to solve the zero displacement boundary problem. All the seven players would have liked to participate in our match but only two of them got the chance. Many other boundary problems can be posed for the elastic rectangle.

Hence, there are many possibilities for contests between Fourier methods and we have just proposed to the reader how to arrange one, hoping (s)he liked the idea and will let the Fourier methods either play or decide the matches as well – in spite of their age and a the little bit of schizophrenia in boundary condition satisfaction.

**Acknowledgments.** We express our gratitude to Professor Viacheslav Meleshko from Kiev National Taras Shevchenko University for making available to us his paper (Meleshko, 1995). This work was supported by Science and Technology Assistance Agency under the contract No. APVT-51-002804 and by VEGA grant agency under projects No. 2/3057/23 and 2/3004/23.

## References

Koialovich B. M., 1930: Studies on the infinite systems of the linear equations (in Russian). *Izv. Fiz. Mat. Inst. Steklova*, **3**, 41–167.

- Meleshko V. V., 1995: Equilibrium of elastic rectangle: Mathieu-Inglis-Pickett solution revisited. *J. Elasticity*, **40**, 207–238.
- Meleshko V. V., 1997: Bending of an elastic rectangular clamped plate: exact versus ‘engineering’ solutions. *J. Elasticity*, **48**, 1-50.
- Meleshko V. V., Gomilko A. M., 1997: Infinite systems for a biharmonic problem in a rectangle. *Proc. R. Soc. Lond. A*, **453**, 2139–2160.
- Rekach V. G., 1977: Instructions for the solution of problems of elasticity theory. 2<sup>nd</sup> ed. (in Russian). *Vyshshaya Shkola*, Moscow, 216 p.